Supporting Information

S1. Potential local aerosol sources at C1 and S1

While Graciosa Island and the location for C1 were selected due to the remote location and minimal population, the Graciosa regional airport is nearby. The airport regularly hosts two flights a day throughout the year, with one in the late morning or early afternoon and the other in the late afternoon. The largest nearby town is Santa Cruz, which is located ~1.8 km to the southeast of C1 with a population of ~1000. We identify potential local aerosol and trace gas sources associated with the airport and other local activities that may be relevant ENA spatially on a satellite image of the northeast section of Graciosa Island (Fig. S1).

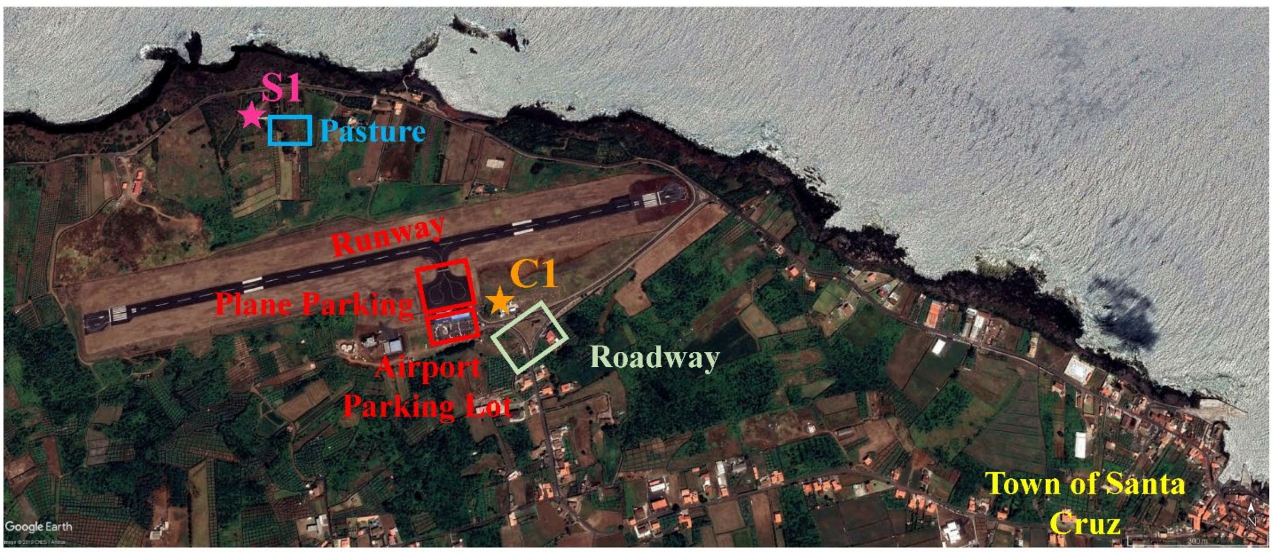

Figure S1. Satellite image with potential aerosol sources identified in the area surrounding ENA on Graciosa Island (© Google Earth).

The airport runway is located 116 m north of C1, spanning from the west to the northeast with regards to C1. The terminal building with one gate is located to the west. The airport parking lot is southwest of C1 and the aircraft parking area is to the west. The town of Santa Cruz is connected to the airport through a road to the east and south of C1.

S1 was located on the other side of the airport runway with respect to the location of C1. As such, the runway is located to the south of S1, spanning from the southwest to the southeast. A rural road that runs close to the shoreline is located to the north. An additional potential source at S1 includes a pasture where cows have been occasionally observed that is located to the east and southeast. A mobile diary unit with a diesel engine has also been observed on occasion in operation in association with the cows and the pasture. When present, the mobile dairy has been observed to operate two times a day for about an hour each time.

Identifying local aerosols at ENA based on proximity and wind direction of the source relative to the measurement site is complex since the sources originate over a wide variety of wind directions. We have attempted to summarize the known potential local aerosol sources in Table S1 as a function of their primary wind direction with regard to the locations of C1 and S1. Four nearby potential aerosol sources were identified at C1: the airport runway from the west to northeast, the road that connects Santa Cruz to the airport from east to south, the airport parking lot to the southwest, the airplane parking area to the west. At S1, the airport runway spans from the east to south and the rural road spans from the west to northeast. These were the two closest potential aerosol sources at S1. Additional potential sources identified near S1 included the pasture from the southeast to south and the decommissioned land fill with active vents to the southwest.

Table S1. Potential aerosol sources identified at ENA as a function of wind direction at C1 and S1.

Wind Direction	**Potential Aerosol Sources near ENA**	
	C1	**S1**
N	Airport runway	Rural road
NE	Airport runway	Rural road
E	Road	Airport runway, Rural road, Pasture
SE	Road	Airport runway, Pasture, Airplane and car parking, Road
S	Road	Airport runway
SW	Airport parking lot	Airport runway, Decommissioned landfill
W	Airport runway, Airplane parking	Rural road
NW	Airport runway	Rural road

Throughout this paper, activities associated with the Graciosa airport that may impact aerosol measurements at ENA are collectively referred to as airport operations. Four known potential sources have been identified: aircraft assistance, runway maintenance, airport parking lot, road to the airport. While this is by no means an exhaustive list, further details on these known potential local aerosol sources at ENA are detailed here. Diesel engine vehicles assist aircraft operations before, during, and after landing and take-off. They assist with the loading and unloading of passengers and luggage during all stages before, during, and after the plane's time on the ground. Large vehicles with diesel engines are typically driven and parked several times daily in open spaces designated for plane loading and unloading to maintain the runway and in front of the airport terminal building. Once a day, between approximately 7:45 and 8:30 UTC, three trucks leave the warehouse west of the airport terminal building, and travel the length of the runway several times over a period of approximately 20 to 25 minutes before returning to the warehouse. The parking lot to the southwest of the airport is utilized mostly during times when planes are arriving and departing and to a lesser degree throughout the operational period of the airport. External to the airport, but still related, is the road that connects the town of Santa Cruz to the airport through an intersection located between the east and south side of the C1 site. While the area is rural, traffic is generally low, and there are no stoplights, increased traffic is observed before the arrival and after the departure of aircraft at the airport.

S2. Comparison of ENA-AM to the filter developed by Zheng et al. (2018)

We recreated the mask developed by Zheng et al. (2018) and we applied it to N_{tot} one-second data collected during our summer period. After applying the filter to the original one-second data, we averaged the data to a one-minute time base, masking the one-minute periods that included any masked data for comparison with ENA-AM. Figure S2 shows a time series of masked one-minute N_{tot} at C1. We observed that both masks were able to identify the high concentration aerosol events, however ENA-AM removed a lower amount of data.

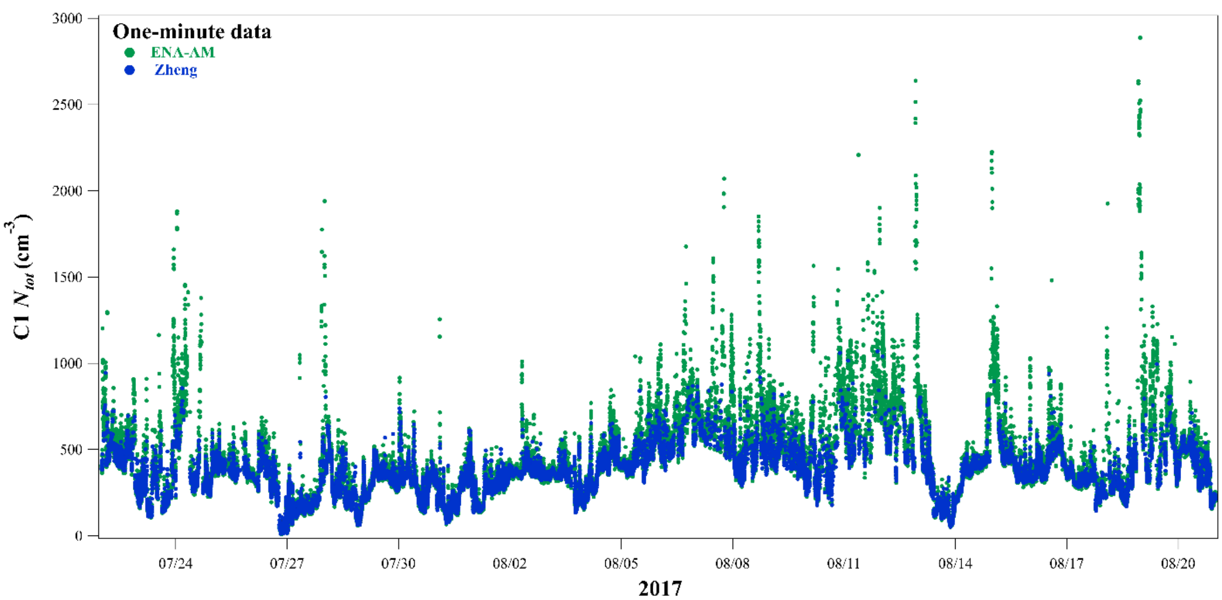

Figure S2. N_{tot} data at C1 in the summer after applying Zheng et al. (2018) method (blue) and ENA-AM (green).

The two masks agreed 68% of the time of the time and a high correlation between the masked datasets was generated (Fig. S3) with a slope of 0.976 and R^2 of 0.988. In this way, the Zheng et al. (2018) method masked a higher amount of data in the one-minute averaged dataset: 41% against the 26% masked by ENA-AM.

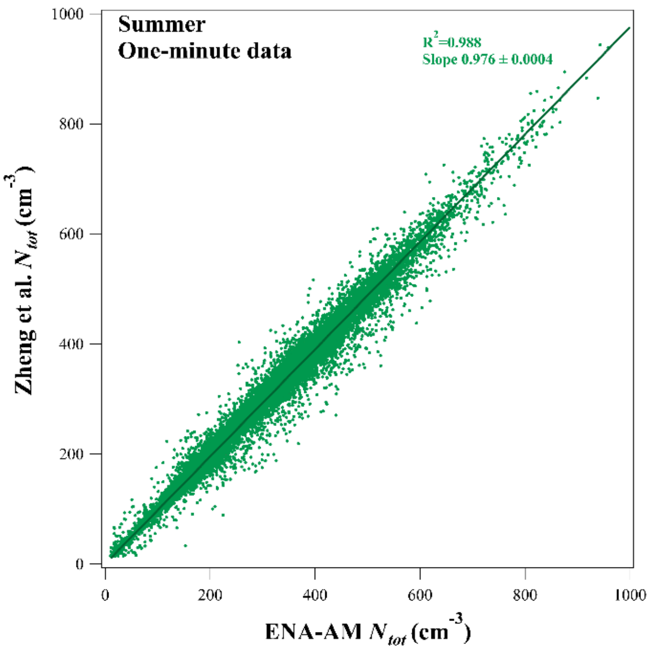

Figure S3. Scatter plot of Zheng et al. (2018) and ENA-AM masked one-minute N_{tot} data at C1 in the summer.

As hourly averages are often used to study seasonal trends and within models, we also investigated the application of both methods to N_{tot} data mapped onto a one-hour time base. Due to the amount of data points masked in N_{tot} one-minute, we averaged the remaining data points within each hour ignoring the masked data points. Without averaging the remaining data within each one-hour time period, 74% of the data for ENA-AM and 96% of the data for Zheng's method would be removed. A slightly lower correlation (R^2 = 0.929 with a slope = 0.876 ± 0.005) was found between the masked one-hour N_{tot} datasets (Fig. S4). This larger deviation between the masks is a result of the lower percentage of data masked by ENA-AM which leads to higher hourly averages in comparison to the other method. The amount of data removed by the Zheng et al. (2018) method in N_{tot} one-hour masked datasets was 4% versus 0.5% removed by ENA-AM.

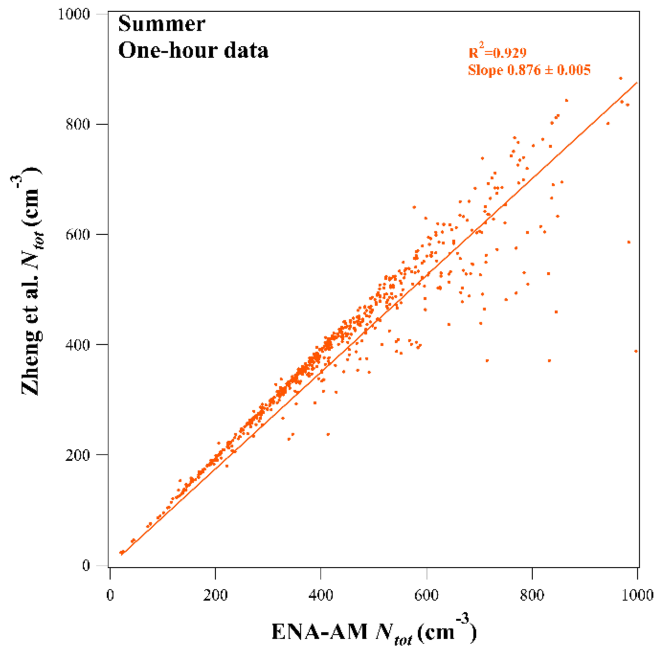

Figure S4. Scatter plot of Zheng et al. (2018) and ENA-AM masked one-hour N_{tot} data at C1 in the summer.